Limits to atom-vapor-based room-temperature photon-number-resolving detection

Elisha S. Matekole,[1,*] Hwang Lee,[1] and Jonathan P. Dowling[1,2,3,4]

[1]*Hearne Institute for Theoretical Physics and Department of Physics and Astronomy, Louisiana State University, Baton Rouge, Louisiana 70803, USA*

[2]*LCAS-Alibaba Quantum Computing Laboratory, CAS Center for Excellence in Quantum Information and Quantum Physics, University of Science and Technology of China, Shanghai 201315, China*

[3]*NYU-ECNU Institute of Physics at NYU Shanghai, 3663 Zhongshan Road North, Shanghai 200062, China*

[4]*National Institute of Information and Communications Technology, Tokyo 184-8795, Japan*

(Received 23 June 2018; published 28 September 2018)

We study the atom-vapor-based photon-number-resolving detection from first principles, including quantum-mechanical treatment of the electromagnetic field. We study a photon detector model that combines coherently controlled absorption of light and resonance fluorescence to achieve photon counting at room temperature. In particular we identify the fundamental limits to this particular scheme of photon detection. We show that there exists a time-energy uncertainty between the incident pulse strength and the time period of the incident pulse. We verify the role of a large ensemble of atoms to boost the efficiency of such a detector.

DOI: 10.1103/PhysRevA.98.033829

I. INTRODUCTION

Photon-number-resolving detectors (PNRD) are crucial to the field of quantum optics, quantum information processing, quantum key distribution [1], quantum teleportation [2], test of Bell's inequalities violations [3], and for linear optics quantum computing [4–6]. Commonly used photon detectors are the bucket or on-off detectors. These detectors can only distinguish between zero and one-or-more photons. Photon-number-resolving detectors typically include avalanche-based photodiodes, such as the visible light photon counters [7,8], two-dimensional arrays of avalanche photodiodes [9,10], time-multiplexed detectors [11–13], photomultipliers [14], and weak avalanche-based PNRD [15]. Most of these detectors have a high dark-count rate at room temperature, and are not sensitive to photon number greater than one. Therefore, they cannot be used in applications that require photon statistics. Another type of PNRD is a transition-edge sensor (TES), which is a superconducting microbolometer. These detectors are highly efficient but they operate at extremely low temperatures and have a slow response time [16–18].

The above state-of-the-art photon detectors rely on getting a detectable signal by converting incident photons to photoelectrons. An alternative approach to resolve photon numbers at room temperature was proposed by James and Kwiat [19]. This scheme is based on coherently controlled absorption of light and projective quantum state measurements. The incident single photon is converted to many photons by resonance fluorescence. Around the same time, another proposal to count photons was proposed by Imamoglu in [20], which combines the techniques of ion-trap quantum state measurements [21] and electromagnetically induced transparency (EIT) [22]. Following along the same lines, Clausen *et al*. proposed a scheme to detect photons based on EIT and resonance fluorescence [23]. However, in the case of trapped ions, typically the system needs to be laser cooled by applying two counterpropagating light beams along the cavity axis. This step is necessary to prepare the system for optical pumping. Also, once the first cycle of detection is completed, a laser repumper is required to cool the system for the next detection cycle.

In this paper we revisit the atom-vapor-based photon detectors at room temperature as proposed in Ref. [19]. A three-level Λ scheme is considered. The detector is prepared using optical pumping to transfer all the atoms in the ground state. The atomic population transfer is achieved by using stimulated Raman adiabatic passage (STIRAP) and the number of photons are detected using a readout laser, which induces fluorescence.

The paper is organized as follows. In Sec. II we will describe the experimental setup. In Sec. III we will describe optical pumping which is essential for preparation of the atomic system to detect photons. Next, we will discuss STIRAP in Sec. IV. We will analyze the STIRAP for both classical and quantized light fields. In Sec. V we will describe the readout step implemented by using resonance fluorescence.

II. EXPERIMENTAL SETUP

The schematic diagram of the proposed photon detector is shown in Fig. 1. We consider an atomic vapor of ^{133}Cs, whose hyperfine structure is shown in Fig. 2(a). The radiation to be detected is incident on the cell containing the atoms in the vapor along with a coupling laser. The photons in the incident radiation excite the atoms to a metastable state $|2\rangle$ as shown in Fig. 2(b). Collisions between atoms and atom-wall collisions can degrade the atom coherence time. Coating the walls of the vapor cell by paraffin coating reduces the effect of atom-wall collisions [24,25]. Filling the vapor cell with inert buffer gas reduces the atomic mean free path,

*esiddi1@lsu.edu

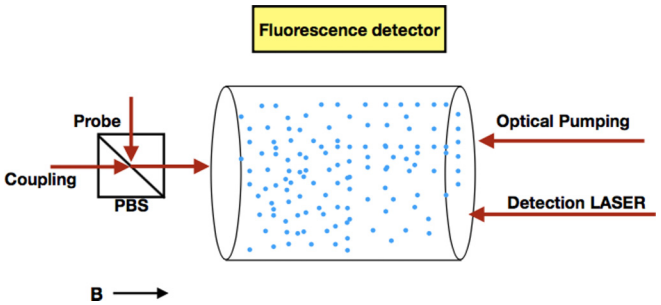

FIG. 1. Schematic diagram of an atom-based photon detector for ^{133}Cs atom. The polarizing beam splitter (PBS) determines the polarizations of the optical field. The applied magnetic-field direction defines the quantization axis.

hence reducing the probability of wall collisions as well as Cs-Cs collisions [26]. If the number of atoms is large enough, the probability that each photon is absorbed by one atom is close to unity. This allows for the use of lower control laser power in the current scheme. Next the atoms in the metastable state are excited using a readout laser that couples only level $|2\rangle$ ($F = 4$), and level $|4\rangle$ ($F = 5$) as shown in Fig. 2, so that only the photons generated by the $|2\rangle$–$|4\rangle$ transition are counted using photon detection imaging, hence resolving the original number of incident photons, by counting the number of fluorescing atoms.

III. OPTICAL PUMPING

Optical pumping is required for the initialization of the photon detector by transferring all atomic population from $|2\rangle$ into the ground state $|1\rangle$ as shown in Fig. 3(a). Initially we assume that both levels $|1\rangle$ and $|2\rangle$ have equal atomic

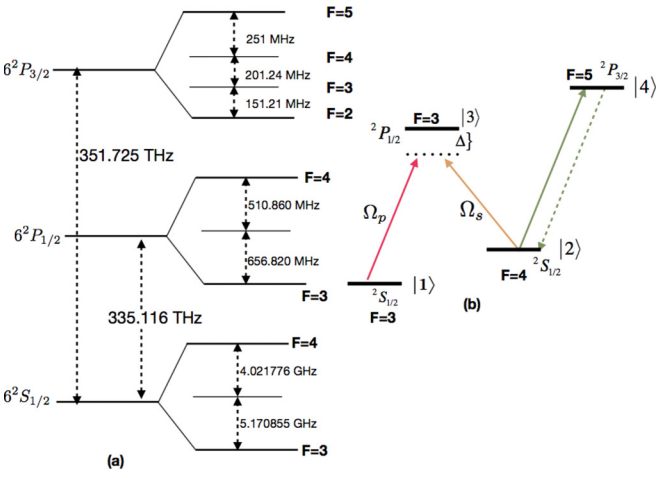

FIG. 2. (a) Energy-level diagram of ^{133}Cs showing the hyperfine structure and the D_1, and D_2 transition [27]. (b) The three-level lambda (Λ) system showing the relevant energy levels for the detector. First an ensemble of atoms is prepared in level $|1\rangle$ via optical pumping. Then the atoms in level $|1\rangle$ are excited to level $|2\rangle$ by absorption of photons in the probe field with the help of coupling laser between levels $|1\rangle$ and $|3\rangle$. Finally the atoms in level $|2\rangle$ are detected via fluorescence between levels $|2\rangle$ and $|4\rangle$.

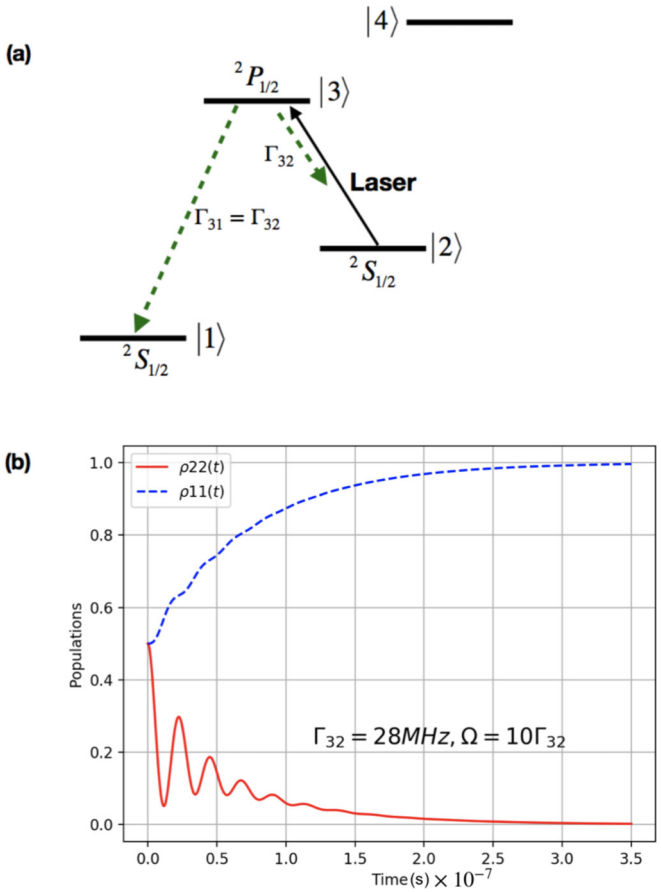

FIG. 3. (a) Initialization of the photon-number detector by pumping all the atomic population from level $|2\rangle$ to level $|1\rangle$. Levels $|2\rangle$ and $|3\rangle$ are coupled by a classical laser. The atoms from level $|2\rangle$ get transferred to level $|1\rangle$ via level $|3\rangle$. (b) Population evolution of levels $|1\rangle$ and $|2\rangle$ as a function of time for a three-level ^{133}Cs atom. Initially both levels $|1\rangle$ and $|2\rangle$ contain equal number of atoms. When the laser field is applied between levels $|3\rangle$ and $|2\rangle$, atoms from $|2\rangle$ get excited to $|3\rangle$ and spontaneously decay to level $|1\rangle$, with a decay rate Γ_{32}. We have considered zero detuning.

population. Complete optical pumping is important as any atoms not transferred from $|2\rangle$ to $|1\rangle$ would lead to spurious detection at the fluorescence stage. The interaction Hamiltonian of a single three-level atom for the optical pumping technique is given as

$$\hat{H}_{\rm int} = -\frac{\hbar}{2}[\Omega e^{-i\Delta t}|3\rangle\langle 2| + |2\rangle\langle 3|\Omega e^{i\Delta t}], \tag{1}$$

where levels $|2\rangle$ and $|3\rangle$ are coupled by a classical laser with Rabi frequency Ω and Δ represents detuning. We obtain the equations of motion in the rotating-wave frame, using the master equation,

$$\dot{\rho_{22}} = \frac{\Omega}{2i}(\rho_{23} - \rho_{23}^*) + \Gamma_{32}\rho_{33}, \tag{2}$$

$$\dot{\rho_{33}} = -\frac{\Omega}{2i}(\rho_{23} - \rho_{23}^*) - 2\Gamma_{32}\rho_{33}, \tag{3}$$

$$\dot{\rho_{23}} = -\gamma_{32}\rho_{23} + \frac{i\Omega}{2}(\rho_{33} - \rho_{22}), \tag{4}$$

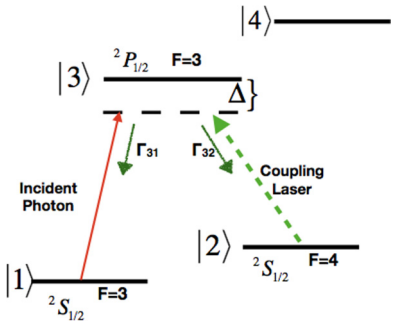

FIG. 4. Photons in the incident pulse are absorbed by atoms in level $|1\rangle$, which are excited to level $|2\rangle$ with the assistance of coupling laser. Γ_{31} and Γ_{32} are the spontaneous decay rates from level $|3\rangle$ to levels $|1\rangle$ and $|2\rangle$, respectively. The detuning between $|3\rangle$ and the incident fields is given by Δ.

where ρ_{ij} are the matrix elements of the density operator, Γ_{ij} is the spontaneous decay rate from level $|i\rangle$ to $|j\rangle$, and γ_{ij} represents the coherence decay rates. Also, we have assumed the detuning $\Delta = 0$. We plot the time evolution of the population in levels $|1\rangle$ and $|2\rangle$ in Fig. 3(b). The time taken for all the population to be transferred in $|1\rangle$ is of the order of 0.35 μs. Once all the atoms are pumped to level $|1\rangle$, we are ready for the next step of detecting photons.

IV. STIRAP

A. Classical STIRAP

The second step of the atom-based photodetection is STIRAP, which is used to transfer population between two atomic levels via an intermediate state [28]. Here we consider a two-photon Raman excitation to level $|2\rangle$. The probe field (containing the photons to be detected) along with a strong-coupling laser field is introduced in the cell containing the atoms. The interaction Hamiltonian for a single three-level atom describing the STIRAP process is

$$\hat{H}_{\rm int} = -\frac{\hbar}{2}[\Omega_p(t)\hat{\sigma}_{31}e^{i\Delta t} + \Omega_s(t)\hat{\sigma}_{32}e^{i\Delta t} + \text{H.c.}]. \quad (5)$$

$\hat{\sigma}_{ij} = |i\rangle\langle j|$ is the atomic projection operator ($i, j = 1, 2, 3$). Ω_p and Ω_s represent the Rabi frequency of the photon and coupling lasers, respectively; Δ represents the detuning of the lasers from the transition frequencies ω_{31} and ω_{32}.

We consider the well-known counterintuitive pulse sequence in this analysis. (See Fig. 4.) First the Stokes pulse is on, such that all the population is in level $|1\rangle$ at some initial time (t_i). Then the probe pulse is on, driving the transition from level $|1\rangle$ to $|2\rangle$ via $|3\rangle$ at final time (t_f). The time dependence of the Rabi frequency is controlled by suitably delayed laser pulses given as

$$\Omega_s(t) = \Omega_s(0)e^{-\frac{(t+\tau)^2}{2T^2}},$$
$$\Omega_p(t) = \Omega_p(0)e^{-\frac{(t-\tau)^2}{2T^2}}, \quad (6)$$

where $\Omega_p(0)$ and $\Omega_s(0)$ represent the maximum amplitude of the Rabi frequency of the probe and coupling lasers. T represents the time duration of the two pulses and τ represents the time delay.

Using the master equation, we obtain the following equations of motion for the given interaction Hamiltonian:

$$\dot{\rho}_{11}(t) = \frac{i\Omega_p(t)}{2}[\rho^*_{13}(t) - \rho_{13}(t)] + \Gamma_{31}\rho_{33}(t),$$
$$\dot{\rho}_{13}(t) = \left(i\Delta - \frac{\gamma_{31}}{2}\right)\rho_{13}(t) + \frac{i}{2}\Omega_p(t)[\rho_{33}(t) - \rho_{11}(t)] - \frac{i}{2}\Omega_s(t)\rho_{12}(t),$$
$$\dot{\rho}_{22}(t) = -\frac{i\Omega_s(t)}{2}[\rho_{32}(t) - \rho^*_{32}(t)] + \Gamma_{32}\rho_{33},$$
$$\dot{\rho}_{32}(t) = -\left(i\Delta + \frac{\gamma_{32}}{2}\right)\rho_{32}(t) - \frac{i}{2}\Omega_s(t)[\rho_{33}(t) - \rho_{22}(t)] + \frac{i}{2}\Omega_p(t)\rho_{12}(t),$$
$$\dot{\rho}_{12}(t) = \frac{i}{2}\Omega_p(t)\rho_{32}(t) - \frac{i}{2}\Omega_s(t)\rho_{13}(t) - \frac{\gamma_{21}}{2}\rho_{12}(t), \quad (7)$$

where $\Gamma_{31(32)}$ are the spontaneous emission rates out of state $|3\rangle$ to level $|1\rangle(|2\rangle)$. The coherence decay rates are given by γ_{31}, γ_{32}, and γ_{21} [29]. The Doppler shift can cause detuning from the critical two-photon resonance in STIRAP. For a particle with velocity v_k, along the laser propagation direction the shift in the detuning Δ is $\Delta_{\rm eff} = \Delta + kv_k$. The effective detuning from two-photon resonance then becomes $\delta_{\rm eff} = (\Delta_p + kv_k) - (\Delta_s + kv_k)$. In our scheme, the two STIRAP beams are at the two-photon resonance ($\Delta_p = \Delta_s$); the Doppler broadening of the two-photon resonance is essentially canceled, when the two lasers beams copropagate. Also, the Zeeman splitting for the hyperfine state $F = 1$ for a magnetic field of 1 G is 0.7 MHz. This gives $\delta_k(|k_p - k_s|) = 14.6 \times 10^{-3}$, such that $\frac{\delta k}{k_p} \sim 10^{-9}$; hence the Doppler shift is negligible [28,30,31].

Assuming perfect optical pumping as discussed in Sec. II, the initial conditions for the above set of differential equations are $\rho_{11}(0) = 1$ and $\rho_{22}(0) = \rho_{33}(0) = 0$.

In Fig. 5, we consider incident photon and coupling laser pulses of time width 30 ns each. The values of the Rabi frequencies are very large for the transfer of all the atoms from level $|1\rangle$ to $|2\rangle$. However, we need only those atoms that absorb the incident photons to be transferred to level $|2\rangle$. Therefore, we can considerably reduce the Rabi frequencies of the two pulses and, as shown in Fig. 6, get a small probability of transfer of single atom to level $|2\rangle$. This probability is enhanced when an ensemble of atoms is considered. For example, consider the population transfer in Fig. 6, which is of the order of 10^{-10}; this increases to 1% the chance of transferring an atom from $|1\rangle$ to $|2\rangle$ in the presence of 10^8 atoms or approaches unity in an ensemble of 10^{10} atoms or more.

B. Quantized STIRAP

In the quantized picture of the two-photon Raman excitation we consider both the incident photon and the coupling

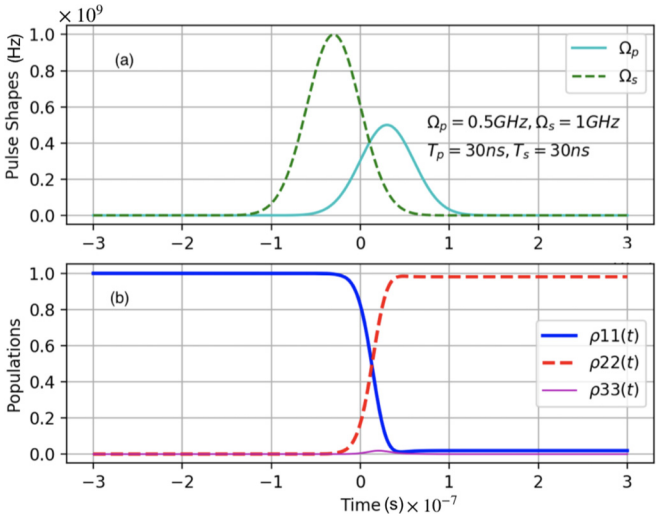

FIG. 5. (a) Pulse shapes for the incident and coupling lasers. The counterintuitive pulse sequence is used. (b) The population evolutions of states $|1\rangle$, $|2\rangle$, and $|3\rangle$ for the counterintuitive pulse sequence, with $\Delta = 0.5$ GHz, $\Gamma_{31} = \Gamma_{32} = 28$ MHz, $\gamma_{31} = \gamma_{32} = 2\Gamma_{31}$, and $\gamma_{21} = 0.001\gamma_{31}$. The time width of the two pulses is $T = 30$ ns. The population is transformed from level $|1\rangle$ to $|2\rangle$ with negligible population in $|3\rangle$. In order to have perfect transfer of population from level $|1\rangle$ to $|2\rangle$, we need very high intensity lasers.

fields to be quantized. The fully quantized interaction Hamiltonian for a single atom in rotating wave frame is given as

$$\hat{H}_{\text{int},Q} = \hbar[g_{13}\hat{a}_p\sigma_{31}e^{i\Delta t} + g_{23}\hat{a}_s\sigma_{32}e^{i\Delta t}] + \text{H.c.}, \quad (8)$$

where $g_{13(23)}$ represents the atom-field coupling constant between levels $|1\rangle(|2\rangle)$ and $|3\rangle$. The atom-field coupling constants are given as $g_{ij} = d_{ij}\sqrt{\omega_{ij}/2\hbar\epsilon_o V}$. The eigenstates of the Hamiltonian can be written as $|1\rangle = |1_A, n_p, n_s, l\rangle$, $|3\rangle = |3_A, n_p - 1, n_s, l\rangle$, and $|2\rangle = |2_A, n_p - 1, n_s + 1, l\rangle$; the subscript A refers to the corresponding atomic level. The number of photons in the incident photon pulse and the coupling laser are given by n_p and n_s, respectively, and l represents the photon number found in the readout laser, which we will discuss in Sec. IV.

The equation of motions for the fully quantized interaction Hamiltonian are given as

$$\begin{aligned}
\dot{\rho}_{11}(t) &= ig_{13}[\rho_{13}(t) - \rho_{13}^*(t)]\sqrt{n_p} + \Gamma_{31}\rho_{33}(t),\\
\dot{\rho}_{13}(t) &= \left(i\Delta - \frac{\gamma_{13}}{2}\right)\rho_{13}(t) + i\sqrt{n_s+1}g_{23}\rho_{12}(t)\\
&\quad - i\sqrt{n_p}g_{13}[\rho_{33}(t) - \rho_{11}(t)],\\
\dot{\rho}_{22}(t) &= -ig_{23}\sqrt{n_s+1}[\rho_{32}(t) - \rho_{32}^*(t)] + \Gamma_{32}\rho_{33}(t),\\
\dot{\rho}_{32}(t) &= -\left(i\Delta + \frac{\gamma_{23}}{2}\right)\rho_{32}(t) - i\sqrt{n_p}g_{13}\rho_{12}(t)\\
&\quad + i\sqrt{n_s+1}g_{23}[\rho_{33}(t) - \rho_{22}(t)]. \quad (9)
\end{aligned}$$

In Fig. 7 we plot the population evolution of levels $|1\rangle$ and $|2\rangle$, for a counterintuitive pulse sequence of incident photon fields and the coupling laser. Here, we find that the probability of the atom being excited to level $|2\rangle$ is unity if both the incident and coupling fields contain a large number of photons. This implies that we cannot use this technique for a single- or few-photon detection.

Since, we want only those atoms to be transferred to level $|2\rangle$ that absorb the incident photons, we do not need a perfect population transfer from $|1\rangle$ to $|2\rangle$. In Fig. 8, we consider the case of a single incident photon and a coupling field with only 50 photons. Both the fields have equal time duration of 30 ns. We find that the probability of transferring the single atom from $|1\rangle$ to $|2\rangle$ is only 10^{-10}. This number can be enhanced when we consider an ensemble containing $10^8 - 10^{10}$ atoms.

Another way to achieve complete population transfer from $|1\rangle$ to $|2\rangle$ for the case of single- or few-photon incident field

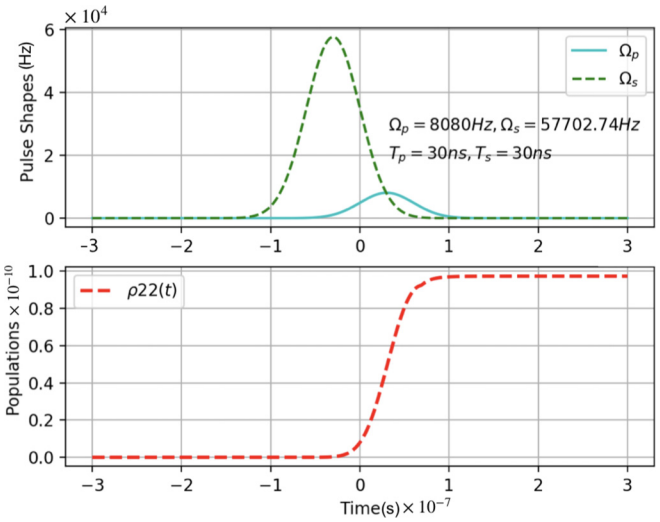

FIG. 6. Population evolution in level $|2\rangle$ for photon and Raman pulses, with a time period of 30 ns. We have set $\Gamma_{31} = \Gamma_{32} = 28$ MHz, $\gamma_{31} = \gamma_{32} = 2\Gamma_{31}$, and $\gamma_{21} = 0.001\gamma_{31}$.

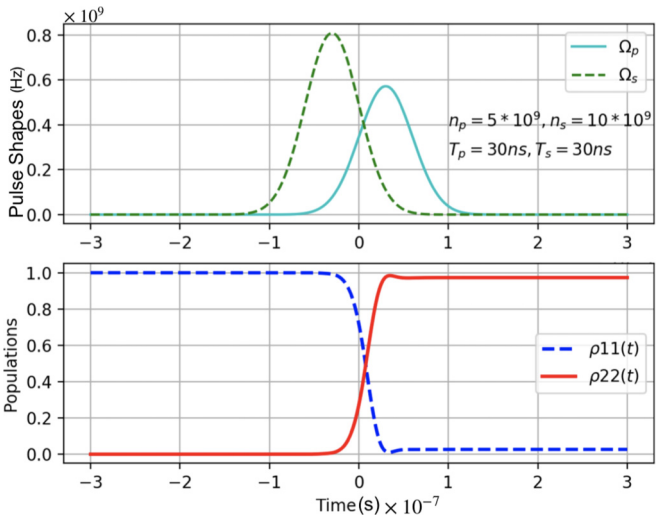

FIG. 7. Population evolution in level $|2\rangle$ for photon and Raman pulses of time period $T = 30$ ns. The number of photons required to complete the population transfer from $|1\rangle$ to $|2\rangle$ in the photon field are 5×10^9, and those in the Raman pulse are 10^{10}.

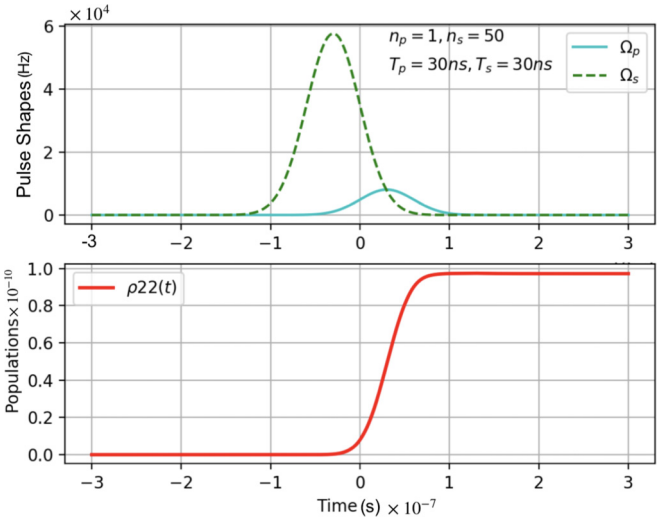

FIG. 8. Population evolution for single-photon pulse and Raman pulse with 50 photons; both pulses have a time period of 30 ns. The value of the atom-field coupling is given as $g_{13} = 4040.83$ Hz and $g_{23} = 4040.771$ Hz. The decay rates are $\Gamma_{31} = \Gamma_{32} = 28$ MHz, $\gamma_{31} = \gamma_{32} = 2\Gamma_{31}$, and $\gamma_{21} = 0.001\gamma_{31}$.

is to increase the time duration of the incident and coupling pulses. We would like to point out that there exists a hitherto hidden energy-time uncertainty in the STIRAP process. If we increase the time period of pulses, then we need less energy to drive the transitions as shown in Fig. 9. If we consider a pulse of time period 1000 s, then the distance the pulse is distributed is 3×10^8 K m. This distance is even greater than the distance between the Earth and the Moon, which is 384 400 K m. Hence it is not feasible to have pulses of such large durations.

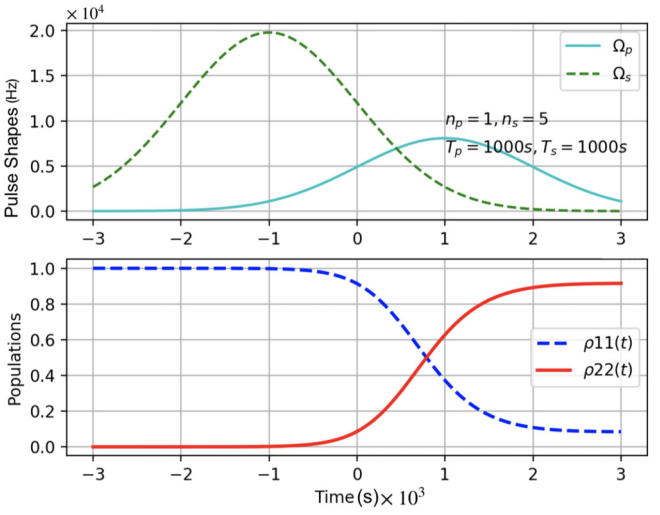

FIG. 9. Population evolution for single photon pulse and Raman pulse with five photons; both pulses have a time period of 1000 s. The value of the atom-field coupling is given as $g_{13} = 4040.83$ Hz and $g_{23} = 4040.771$ Hz. The decay rates are $\Gamma_{31} = \Gamma_{32} = 28$ MHz, $\gamma_{31} = \gamma_{32} = 2\Gamma_{31}$, and $\gamma_{21} = 0.001\gamma_{31}$.

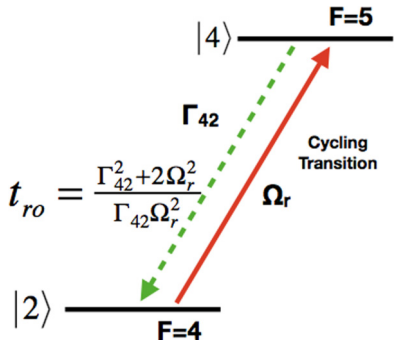

FIG. 10. Readout laser couples only levels $|2\rangle$ and $|4\rangle$ such that only the atoms excited to level $|2\rangle$ are detected. The number of photons are counted by counting the atoms in $|2\rangle$, via the cycling transition between $|4\rangle$ and $|2\rangle$.

V. RESONANCE FLUORESCENCE

The metastable state $|2\rangle$ is chosen so that it can undergo a cycling transition with another atomic state $|4\rangle$. The number of atoms excited to level $|2\rangle$ are detected by employing a cycling transition between $|2\rangle$ and $|4\rangle$, i.e., atoms in level $|2\rangle$ will get excited to $|4\rangle$ via the readout laser and will spontaneously decay back to level $|2\rangle$ only. The number of photons emitted will be proportional to the number of atoms in level $|2\rangle$, hence resolving the photon number in the incident radiation. The time taken for detecting a single photon using this method can be obtained by solving the equation of motion for the density matrices in steady state and the readout laser time is given by $t_{\rm ro} = (\Gamma_{42}^2 + 2\Omega_r^2)/\Gamma_{42}\Omega_r^2$. The quantized version of resonance fluorescence yields the same steady-state result, except that the Rabi frequency is $\Omega_r = 2g_r\sqrt{l}$, where g_r represents the coupling constant and l is the number of photons in the readout laser. The numerical value of $t_{\rm ro}$ is 0.052 μs for ^{133}Cs atoms. (See Fig. 10.)

VI. CONCLUSION

In this paper we have investigated the atom-based photon-number-resolving detectors in detail. We have analyzed both the classical and quantum models for STIRAP. We considered the case of single atom and found that sufficiently strong probe and coupling lasers are required to transfer a single atom from the ground state to the metastable state with probability one. Therefore, an extremely weak probe pulse consisting of one or few photons cannot suffice to excite the population in the ground state to the metastable state. In other words the probability to excite a single atom to the metastable state is extremely small. However, this probability can be enhanced if we consider an ensemble of atoms, since we need only those atoms excited that absorb the incident photons to be able to resolve photon number at the readout stage. This enables the use of low-intensity laser pulses. Also, there exists a trade off between the magnitude of Rabi frequencies of the probe and coupling lasers and the pulse duration. If the pulse duration increases, then the magnitude of the Rabi frequencies decreases and vice versa. Large duration pulses imply photon wave packet spread out over large distances, which is not a desirable feature.

Another source of having false photon detections (dark counts) can be due to imperfect optical pumping, i.e., if some atoms still remain in the metastable state at the initialization stage. Hence, based on our analysis, if we can have an ensemble of atoms at the STIRAP stage and implement complete optical pumping, the above technique can be used to resolve photon number at room temperature.

ACKNOWLEDGMENTS

The authors would like to acknowledge the Air Force Office of Scientific Research, The Army Research Office, The Defense Advanced Research Projects Agency, DETECT program, The National Science Foundation, and The Northrop Grumman Corporation.

[1] C. H. Bennett, F. Bessette, G. Brassard, L. Salvail, and J. Smolin, J. Cryptology **5**, 3 (1992); A. K. Ekert, J. G. Rarity, P. R. Tapster, and G. Massimo Palma, Phys. Rev. Lett. **69**, 1293 (1992).

[2] D. Bouwmeester, J.-W. Pan, K. Mattle, M. Eible, H. Weinfurter, and A. Zeilinger, Nature (London) **390**, 575 (1997).

[3] A. Aspect, P. Grangier, and G. Roger, Phys. Rev. Lett. **49**, 91 (1982); A. Aspect, J. Dalibard, and G. Roger, *ibid.* **49**, 1804 (1982); G. Weihs, T. Jennewein, C. Simon, H. Weinfurter, and A. Zeilinger, *ibid.* **81**, 5039 (1998).

[4] E. Knill, R. Laflamme, and G. J. Milburn, Nature (London) **409**, 46 (2001).

[5] P. Kok, W. J. Munro, K. Nemoto, T. C. Ralph, J. P. Dowling, and G. J. Milburn, Rev. Mod. Phys. **79**, 135 (2007).

[6] C. Simon, H. de Riedmatten, M. Afzelius, N. Sangouard, H. Zbinden, and N. Gisin, Phys. Rev. Lett. **98**, 190503 (2007).

[7] E. Waks, E. Diamanti, B. C. Sanders, S. D. Bartlett, and Y. Yamamoto, Phys. Rev. Lett. **92**, 113602 (2004).

[8] E. Waks, K. Inoue, W. D. Oliver, E. Diamanti, and Y. Yamamoto, IEEE J. Sel. Top. Quantum Electron. **9**, 1502 (2003).

[9] K. Yamamoto, K. Yamamura, K. Sato, T. Ota, H. Suzuki, and S. Ohsuka, IEEE Nucl. Sci. Symp. Conf. Record **2**, 1094 (2006).

[10] L. A. Jiang, E. A. Dauler, and J. T. Chang, Phys. Rev. A **75**, 062325 (2007).

[11] D. Achilles, C. Silberhorn, C. Śliwa, K. Banaszek, and I. A. Walmsley, Opt. Lett. **28**, 2387 (2003).

[12] M. J. Fitch, B. C. Jacobs, T. B. Pittman, and J. D. Franson, Phys. Rev. A **68**, 043814 (2003).

[13] D. Achilles, C. Silberhorn, and I. A. Walmsley, Phys. Rev. Lett. **97**, 043602 (2006).

[14] G. Zambra, M. Bondani, A. S. Spinelli, F. Paleari, and A. Andreoni, Rev. Sci. Instrum. **75**, 2762 (2004).

[15] B. E. Kardynal, Z. L. Yuan, and A. J. Shields, Nat. Photon. **2**, 425 (2008).

[16] A. E. Lita, A. J. Miller, and S. W. Nam, Opt. Express **16**, 3032 (2008).

[17] A. E. Lita, A. J. Miller, and S. W. Nam, J. Low Temp. Phys. **151**, 125 (2008).

[18] B. Calkins, P. L. Mennea, A. E. Lita, B. J. Metcalf, W. S. Kolthammer, A. Lamas-Linares, J. B. Spring, P. C. Humphreys, R. P. Mirin, J. C. Gates, P. G. R. Smith, I. A. Walmsley, T. Gerrits, and S. W. Nam, Opt. Express **21**, 22657 (2013).

[19] D. F. V. James and P. G. Kwiat, Phys. Rev. Lett. **89**, 183601 (2002).

[20] A. Imamoğlu, Phys. Rev. Lett. **89**, 163602 (2002).

[21] M. A. Rowe, D. Kielpinski, V. Meyer, C. A. Sackett, W. M. Itano, C. Monroe, and D. J. Wineland, Nature (London) **409**, 791 (2001).

[22] K. J. Boller, A. Imamoğlu, and S. E. Harris, Phys. Rev. Lett. **66**, 2593 (1991); S. E. Harris, Phys. Today **50**, 36 (1997); M. D. Lukin and A. Imamoğlu, Nature (London) **413**, 273 (2001).

[23] C. Clausen, N. Sangouard, and M. Drewsen, New J. Phys. **15**, 025021 (2013).

[24] M. A. Bouchiat and J. Brossel, Phys. Rev. **147**, 41 (1966).

[25] M. T. Graf, D. F. Kimball, S. M. Rochester, K. Kerner, C. Wong, D. Budker, E. B. Alexandrov, M. V. Balabas, and V. V. Yashchuk, Phys. Rev. A **72**, 023401 (2005).

[26] W. Franzen, Phys. Rev. **115**, 850 (1959).

[27] D. A. Steck, http://steck.us/alkalidata.

[28] N. V. Vitanov, A. A. Rangelov, B. W. Shore, and K. Bergmann, Rev. Mod. Phys. **89**, 015006 (2017).

[29] M. Fleischhauer, A. Imamoglu, and Jonathan P. Marangos, Rev. Mod. Phys. **77**, 633 (2005).

[30] M. S. Feld and A. Javan, Phys. Rev. **177**, 540 (1969).

[31] B. W. Shore, Adv. Opt. Photon. **9**, 563 (2017).